International Journal of Multidisciplinary Science and Innovation (IJMSI)
International Conference on Advances in Physical, Chemical and Mathematical Sciences for Sustainable Development
Organized by
D.M.S. Mandal's Bhaurao Kakatkar College, Belgaum, Karnataka, India
Website: https://ijmsi.in/
ISSN: 3107-5754 I Vol. 2, Special Issue 1, 2026 I Page No.: 129-138

Research

Numerical Analysis of Heat and Mass Transfer through MHD Casson Fluid with Variable properties over a Permeable Elongating Sheet

Vishwanath B. Awati*[1], Sachin S. Muchandi[2]
Department of Mathematics, Rani Channamma University, Belagavi-591156, INDIA

Corresponding Author:
Vishwanath B. Awati

Email: *awati.vb@rcub.ac.in, sachinmuchandi456@gmail.com*

DOI: *10.62896/ijmsi.2.s1.16*

Conflict of interest: *NIL*

Article History
Received: 08/06/2026
Accepted: 16/06/2026
Published: 20/06/2026

Abstract:
The paper presents, the heat and mass transfer characteristics of variable viscous MHD Casson fluid flow over a nonlinear permeable stretching sheet under viscous dissipation with suction. The leading coupled nonlinear partial differential equations (PDE's) are exercised into coupled self-similar system of nonlinear ordinary differential equations (ODE's) through suitable similarity variables. These equations are solved numerically by utilizing Keller box method (KBM). The impact of various flow parameters involved in the physical problem are discussed in detail. The attained results are presented in the form of tables and graphs. The analysis reveals that flow is prominently influenced by the physical parameters and also attained results are compared with the earlier published findings which are comparable. The flow is accelerated with variable viscosity and decelerated with suction parameter.

Keywords: Nonlinear stretching; Casson fluid; Variable viscosity; Viscous dissipation; Keller box method.

1. Introduction

Boundary layer flow over a stretching surface is frequently encountered in most of the engineering fields. The flow generated by a stretching boundary is particularly significant in the extrusion processes within the plastic and metal industries [1]. Flow and heat transfer phenomena have valuable applications in technological processes such as the production of polymer films of thin sheets. Sakiadis [2] studied the two-dimensional boundary layer flow problems. Crane [3] analysed the flow of an incompressible viscous fluid over an elastic sheet. Crane's work was later expanded by other researchers to Newtonian and non-Newtonian boundary layer flows, with different velocities and thermal boundary conditions. Abel et al. [4] examined the flow and heat transfer in power-law fluid over a stretching sheet with variable thermal conductivity and non-uniform heat source by using the Keller box method [5]. The study of heat transfers due to a continuously stretching surface through an ambient fluid is a key area of current research. Mukhopadhyay and Anderson [6] discussed the slip effects on heat transfer for the interpretation of flow over an unsteady stretching sheet. Ishak et al. [7] scrutinized the steady MHD flow towards a vertical permeable sheet with prescribed heat flux. Fang et al. [8] investigated the effects of slip and magnetic parameters on mass transfer and provided the closed-form solution of governing Navier-Stokes equations. Awati et al. [9] inspected the heat and mass transfer of convective steady-state boundary layer flow of nanofluid over a nonlinear stretching surface using Haar wavelet collocation method (HWCM). Turkyilmazoglu [10] discussed the second-order slip effects on MHD flow and heat transfer over absorptive stretching/shrinking surfaces under innumerable physical situations.

Further, Van Gorder et al. [11] studied the effects of slip and suction parameters on fluid velocity and tangential stress. Presently, thermal loss is the toughest challenge faced by a lot of automobile industries, microelectronics, manufacturing processes, etc. The intensification in temperature results into a rise in transport phenomena, and hence it affects the heat transfer at the wall. Thus, it is important to examine various fluid properties to analysed the heat transfer and flow rates. Awati and Bujurke [12] explored the analytical solution of viscous fluid flow problem with suction/injection effects. Prasad et al. [13] analysed the heat transfer and visco-elastic fluid flow along with stretched nonlinear surfaces in a porous medium utilizing the fourth-order Runge-Kutta method together with a shooting iteration scheme. Awati and Mahesh [14] considered the convective two-dimensional boundary layer flow over a semi-infinite static and moving horizontal plate by using the Haar wavelet method. In another flow problem, Abbas and Hayat [15] discussed the heat transfer of stagnation point flow over a nonlinear stretching surface. Liao [16] determined the solution of boundary layer flow over an impermeable stretching plate. Further, Liao [17] extended the work to permeable stretching plate with suction and injection cases. Uddin et al. [18] revealed the aspects of boundary layer flows over a non-isothermal stretching surface, incorporating porosity, slip, and magnetic effects. Prasad et al. [19] analysed the variable viscous nanofluid flow over a slender elastic sheet through optical homotopy analysis method (OHAM). Awati et al. [20] studied the flow characteristics of MHD Williamson nanofluid passing through porous medium. Ramya et al. [21] discussed the boundary layer flow and heat transfer of a viscous nanofluid with the effect of thermal wall slip using Keller box method. Mustafa et al. [22] reported the analytical observations of heat transfer analysis of Casson fluid with viscous dissipation in the region of stagnation point towards a stretching sheet. Awati et al. [23] debated the influence of transpiration on MHD nanofluid flow, varying thermophysical parameters via KBM and HWCM. Recently, Awati et al. [24] presented bioconvective MHD-UCM nanofluid flow passing over a nonlinear stretching sheet using KBM and HWCM.

Motivated by the above literature review, in the present paper we studied the flow and heat transfer characteristics of magnetohydrodynamic Casson fluid flow with variable viscosity and viscous dissipation over a nonlinear stretching surface. The governing partial differential equations (PDEs) are simplified by utilizing the suitable similarity variables and attained coupled nonlinear ordinary differential equations (ODEs) are solved by using Keller box and Haar wavelet collocation methods, the obtained results are presented through tables and graphs. The analysis reveals that, the current results follow the earlier published findings and influencing parameters has significant impact on flow and heat transfer.

2. Mathematical formulation

Consider the flow of a variable viscous two-dimensional incompressible fluid passing a permeable ($V_w \neq 0$ see Liao [17]) sheet coinciding with plane $y=0$. Two equal and opposite forces are applied along the x axis so that the wall is stretched with the fixed origin. Let $U_w(x) = cx^n$ is the stretching velocity of the surface, where constant c decides the sheet is of stretching $(c > 0)$ or shrinking $(c < 0)$. Let $V_w(x) = V_0 x^{(n-1)/2}$ is the velocity of a fluid through the permeable sheet, where $V_0 < 0$ corresponds to suction and $V_0 > 0$ is the injection of mass flux.

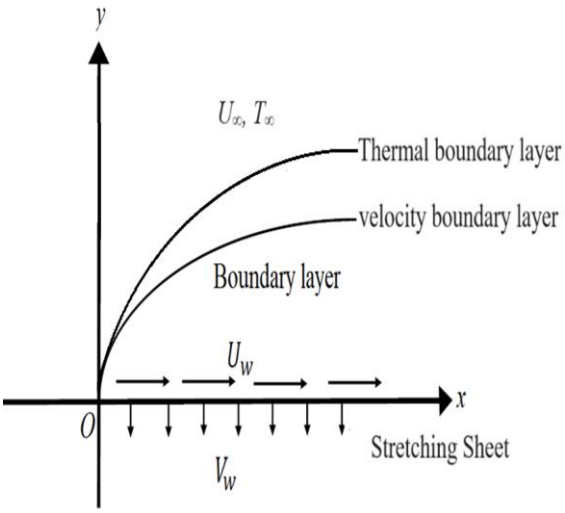

Fig. 1 geometrical representation of flow.

The governing equations comprising continuity, momentum and energy of the flow are given as Cortell [25]

$$\frac{\partial u}{\partial x}+\frac{\partial v}{\partial y}=0, \tag{1}$$

$$u\frac{\partial u}{\partial x}+v\frac{\partial u}{\partial y}=\frac{1}{\rho}\left(1+\frac{1}{\beta}\right)\frac{\partial}{\partial y}\left(\mu\frac{\partial u}{\partial y}\right)-\frac{\sigma B^2(x)u}{\rho}-\frac{\upsilon u}{K_1}, \tag{2}$$

$$u\frac{\partial T}{\partial x}+v\frac{\partial T}{\partial y}=\frac{1}{\rho C_p}\frac{\partial}{\partial y}\left(K(T)\frac{\partial T}{\partial y}\right)+\frac{\upsilon}{\rho C_p}\left(1+\frac{1}{\beta}\right)\left(\frac{\partial u}{\partial y}\right)^2. \tag{3}$$

The pertinent boundary constraints are

$$\left.\begin{array}{lll} u=U_w(x), \quad v=V_w(x), \quad T=T_w & \text{at} & y=0 \\ u\to 0, \qquad T\to T_\infty & \text{as} & y\to\infty \end{array}\right\}, \tag{4}$$

where u and v are the velocity components of fluid along x and y directions respectively. $B(x)$ is the magnetic field defined by $B(x)=B_0x^{(n-1)/2}$, σ denotes electrical conductivity and B_0 is the magnetic constant. ρ is the constant fluid density, C_p is the specific heat. β denotes Casson fluid parameter. T is the fluid temperature and T_w is the constant surface temperature at the wall. In the present analysis, the variable viscosity is considered i.e. μ is assumed to vary as an inverse function of temperature (for details see Lai and Kulacki [26]) given by

$$\mu=\frac{\mu_\infty}{\left[1+\gamma\left(T-T_\infty\right)\right]} \quad \text{i.e.} \quad \mu=\frac{\mu_\infty}{\left[a\left(T-T_r\right)\right]}, \tag{5}$$

where $a=\gamma/\mu_\infty$, T_∞ is the temperature away from the sheet and $T_r=T_\infty-1/\gamma$. Here a and T_r are both constants reflecting thermal property of the fluid whose values depends on reference state and small parameter γ. In general, $a<0$ corresponds to gases and $a>0$ corresponds to liquids. The variable thermal conductivity $K(T)$ is given by

$$K(T)=1+k_\infty\varepsilon\left[\frac{T-T_\infty}{T_w-T_\infty}\right], \tag{6}$$

here ε is the small parameter, k_∞ is the thermal conductivity far away from the sheet [4].

The similarity variables exist for Eqs. (1) to (3), automatically satisfies continuity equation and are given as

$$\psi(x,y)=\sqrt{\frac{2c\upsilon_\infty}{n+1}}f(\eta)x^{\frac{(n+1)}{2}}, \quad \eta=y\sqrt{\frac{(n+1)}{2}\frac{c}{\upsilon_\infty}}x^{\frac{(n-1)}{2}}, \quad \theta(\eta)=\frac{(T-T_\infty)}{(T_w-T_\infty)}. \tag{7}$$

Using the definition of stream function the velocity components can be written as

$$u=U_wf'(\eta) \text{ and } v=-\sqrt{\frac{(n+1)\upsilon_\infty c}{2}}\,x^{\frac{n-1}{2}}\left(f(\eta)+\eta f'(\eta)\left(\frac{n-1}{n+1}\right)\right), \tag{8}$$

where prime indicates the differentiation with respect to η. Using the similarity variables and velocity components defined above, Eqs. (2-3) reduces to

$$\left(1+\frac{1}{\beta}\right)\theta_r\left(\left(\theta_r-\theta\right)^{-1}f''\right)'-\frac{2n}{n+1}\left(f'\right)^2+ff''-\left(Mn+Pt\right)f'=0, \tag{9}$$

$$\frac{1}{Pr}\left[\left(1+\varepsilon_1\theta\right)\theta''+\varepsilon_1\left(\theta'\right)^2\right]+f\theta'+Ec\left(1+\frac{1}{\beta}\right)\theta_r\left(\theta_r-\theta\right)^{-1}\left(f''\right)^2=0. \tag{10}$$

The relevant boundary conditions (4) becomes

$$\left.\begin{aligned} &f(0)=s,\quad f'(0)=1,\quad \theta(0)=1,\\ &f'(\eta)\to 0,\quad \theta(\eta)\to 0 \qquad \text{as} \quad \eta\to\infty, \end{aligned}\right\}. \tag{11}$$

Here, the non-dimensional thermophysical parameters *Pr, Ec, s,* θ_r , Mn and Pt denoting Prandtl number, Eckert number, suction, fluid viscosity, magnetic and porosity parameters respectively and are defined as

$$\left.\begin{aligned} &\Pr=\frac{\upsilon_\infty}{\alpha_\infty},\quad Ec=\frac{U_w^2}{C_p\left(T_w-T_\infty\right)},\quad s=-V_0\sqrt{\frac{2}{c\left(n+1\right)\upsilon_\infty}},\quad \theta_r=\frac{T_r-T_\infty}{T_w-T_\infty}=-\frac{1}{\gamma\left(T_w-T_\infty\right)},\\ &Mn=\frac{2\sigma B_0^2}{\rho c\left(n+1\right)},\qquad Pt=\frac{2\upsilon_\infty B_0^2}{K_1 c\left(n+1\right)B^2}. \end{aligned}\right\} \tag{12}$$

Here $\alpha_\infty=k_\infty/\rho C_p$ is a constant. Utilizing the similarity variables, the interesting dimensionless physical parameters, skin friction coefficients C_f and local Nusselt number Nu_x are given in terms of local Reynolds number (Re_x) as

$$C_f=\sqrt{\frac{2\left(n+1\right)}{\mathrm{Re}_x}}\left(1+\frac{1}{\beta}\right)f''(0),\qquad Nu_x=-\sqrt{\frac{\left(n+1\right)\mathrm{Re}_x}{2}}\theta'(0). \tag{13}$$

Table 1. Comparison table for velocity gradient $-f''\left(0\right)$ for different values of *n*.

		Present Work
n	Cortell [25]	KBM
0	0.62754	0.62763
0.2	0.76676	0.76691
0.5	0.88948	0.88961
0.75	0.95379	0.95379
1	1.00000	1.00000
3	1.14864	1.14864
7	1.21685	1.21690
10	1.23488	1.23490
20	1.25742	1.25747
100	1.27768	1.27682

3. Method of solution

The coupled system of Eqs. (9) -(10) are highly nonlinear ODE's, it is difficult to determine the closed form solution by using analytical method. These equations were solved numerically by using Keller Box method.

3.1 Keller Box method

Keller box method is an elegant numerical method which is the extension of finite difference scheme developed by Keller [5]. It is one of the most adaptive methods for solving nonlinear boundary value problems of various complex geometries. Keller box method involves the discretization of the domain into grid points and solving iteratively for the unknown values at each grid point. Na [27] has

described the detailed procedure of Keller box method for various problems and shows that, this method is particularly useful for the parabolic problems. The principal steps involved in Keller Box method are as follows

i. Transform the system of higher order differential equations into system of first order equations.

ii. The reduced system of first order ODEs, the average and finite difference formula is used in place of dependant variable and its derivative to get the system of nonlinear algebraic equations.

iii. By using Newtons quasi-linearization technique, the system of nonlinear equations can be converted into quasi-linear algebraic system of equations and these equations can be written can be written in matrix form.

iv. Block tri-diagonal elimination technique is used to solve the quasi-linear algebraic systems.

Here initial approximations are made utilizing the boundary conditions and results are obtained with the error estimation of 10^{-5}.

Table 2. Comparison table for temperature gradient $-\theta'(0)$ for different values of n with Pr=1.

			Present Work
Ec	*n*	Cortell [25]	KBM
0.0	0.2	0.61026	0.61032
	0.5	0.59527	0.59538
	1.5	0.57454	0.57471
	3	0.56503	0.56503
	10	0.55496	0.55034

Table 3. Numerical values of $-f''(0)$ and $-\theta'(0)$ for different values of thermophysical parameters for n=5.

θ_r	*Mn*	*Pt*	ε	β	*Pr*	*S*	*Ec*	$f''(0)$	$\theta'(0)$
								KBM	KBM
-∞	0.5	0.5	0.1	1	1	0.5	0.1	-1.23195	-0.89672
-1								-1.90710	-0.72907
-10								-1.31233	-0.78201
-100	0.5							-1.24025	-0.89667
	1.0							-1.34918	-0.89160
	1.5							-1.44899	-0.88678
	2.0	0.5						-1.54168	-0.88216
		1.0						-1.62859	-0.87780
		1.5						-1.71070	-0.87338
		2.0	0.1					-1.78872	-0.86919
			0.2					-1.78871	-0.86222
			0.3					-1.78873	-0.88548
			0.4					-1.78873	-0.89127
			0.1	1				-1.78874	-0.89497
				2				-2.08924	-0.80251
				3				-2.27755	-0.79710
				4				-2.30749	-0.79796
				1	1			-1.78872	-0.86919
					2			-1.78876	-0.87047
					3			-1.78961	-1.39058
					4			-1.79001	-1.82219
					1	1		-1.92776	-0.91562

International Journal of Multidisciplinary Science and Innovation (IJMSI)
International Conference on Advances in Physical, Chemical and Mathematical Sciences for Sustainable Development
Organized by
D.M.S. Mandal's Bhaurao Kakatkar College, Belgaum, Karnataka, India
Website: https://ijmsi.in/
ISSN: 3107-5754 I Vol. 2, Special Issue 1, 2026 I Page No.: 129-138

2		-2.23452	-1.57344
3		-2.57542	-2.41840
5		-3.34029	-4.07457
	1	-3.33830	0.20245
	1.5	-3.33810	1.35442
	2	-3.33786	2.58028
	3	-3.33731	5.13414

4. Results and discussion

The numerical computation were performed to analyse the boundary layer flow problem for different values of physical parameters involved in the physical problem. The nonlinear coupled system of ordinary differential Eqs. (10)-(11) with corresponding boundary constraints (12) are solved by using Keller box method. Table 1 and Table 2 presents the numerical comparison of $f''(0)$ and $\theta'(0)$ values respectively obtained by Keller box method with Cortell [25] which are identical. It shows that, Skin friction coefficient (C_f) decreases and local Nusselt number (Nu_x) increases with increasing values of n. Table 3 illustrates the impact of physical parameters on $f''(0)$ and $\theta'(0)$ with suction. It is examined that, the local Nusselt number increases with increasing values of magnetic parameter Mn. Further the skin friction shows the opposite behaviour with transverse magnetic field. The increase in thermal conductivity parameter (ε) shows an intensification in the resulting surface drag forces and the heat transfer rate. It is noticed that, local Nusselt number increases with increasing thermal conductivity. Table 3 depicts that, Eckert number (Ec) has significant impact on local Nusselt number as sudden increase is observed in Nu_x with increasing values of Ec. Suction parameter (S) has similar effect on C_f and Nu_x, both increases notably with increasing S. It is also witnessed that, both C_f and local Nusselt number are enhanced with higher Prandtl number.

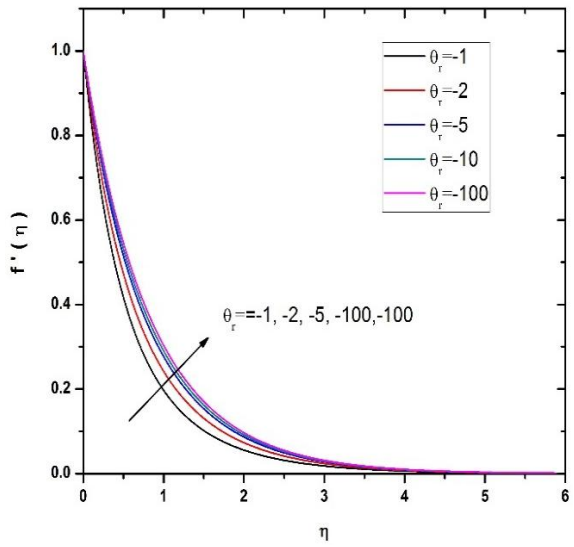

Fig. 2 Imapct of θ_r on velocity profiles.

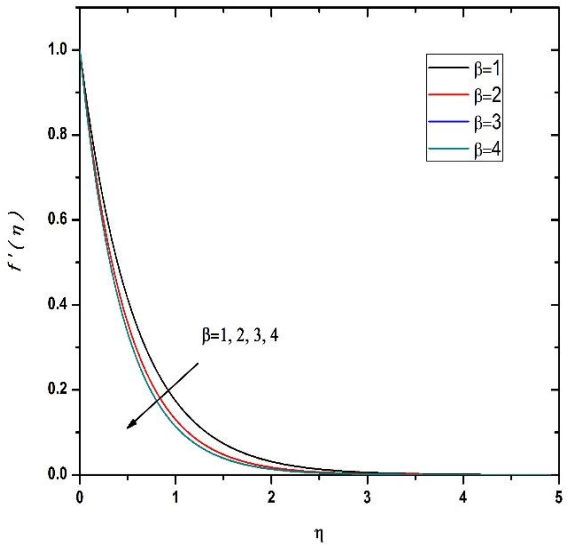

Fig. 3 Impact of β on velocity profiles.

The viscocity of liquids decreases with increasing temparature and increases for gases. This attributes that θ_r is negative for liquids and positive for gases. Hence negative values of θ_r are considered in the present analysis. Fig. 2 demonstrates the effect of θ_r on velocity profiles. It shows that, velocity of the fluid enhances with increasing values of θ_r. Further, the thickness of

boundary layer approaches to zero as $\theta_r \to 0$. Also, it depicts that, both skin friction coefficient and local Nusselt number decreases as θ_r approaches to zero. Fig. 3 shows the Casson fluid parameter (β) has similar effect on velocity profile as flow rate decreases with increasing β. Fig. 4 predicts the effect of suction parameter (S) on velocity of the fluid. It is noticed that, the decrease in velocity profiles with increasing suction parameter which correlates with Bernoulli's phenomena. Similar pattern is observed on heat transfer in Fig 5, it displays diminished temperature profiles for higher values of suction parameter.

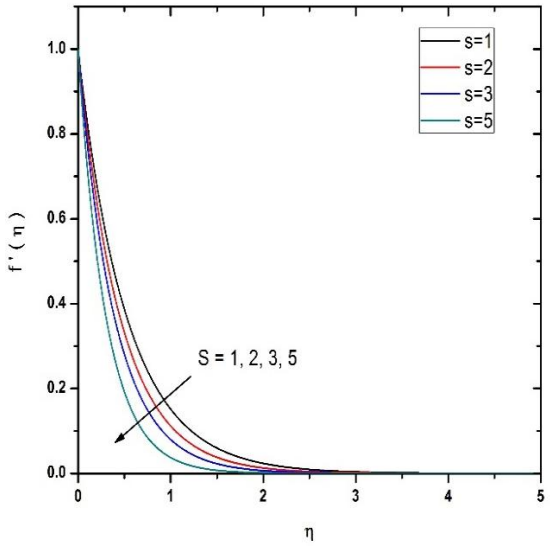

Fig. 4 Imapct of S on velocity profiles.

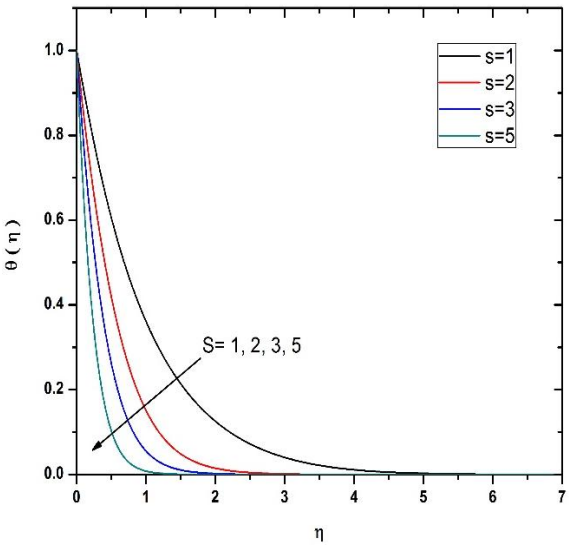

Fig. 5 Impact of S on temparature profiles.

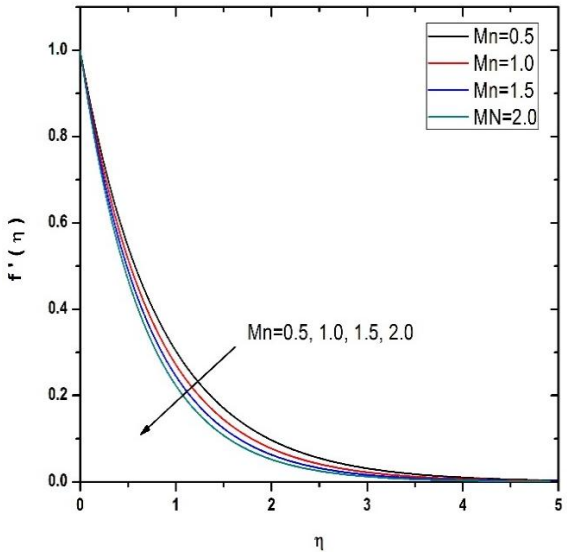

Fig. 6 Imapct of Mn on velocity profiles.

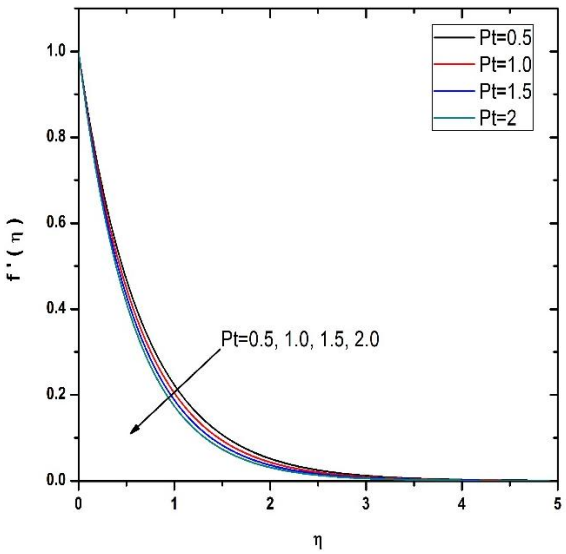

Fig. 7 Impact of Pt on velocity profiles.

Fig. 6 and Fig. 7 exhibits the behaviour of velocity profiles with the change in values of magnetic and porosity parameters respectively. It demonstrates that, the reduced velocity profiles with increase in both magnetic (Mn) and porosity (Pt) parameters. When magnetic field is applied to a Casson fluid, it generates Lorentz force in the perpendicular direction of fluid motion which resists the fluid velocity. Also, in the porous medium fluid must navigate through pores resulting into reduced fluid velocity.

Website: https://ijmsi.in/
ISSN: 3107-5754 I Vol. 2, Special Issue 1, 2026 I Page No.: 129-138

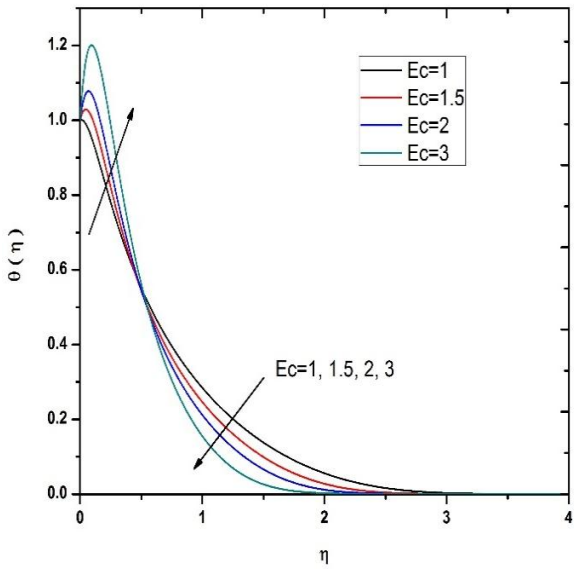

Fig. 8 Imapct of *Ec* on temparature profiles.

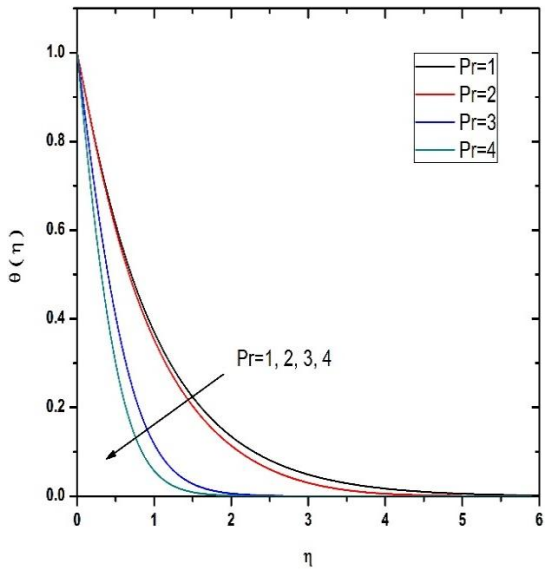

Fig. 9 Impact of *Pr* on temparature profiles.

The dual nature in Fig. 8 highlights the complex relationship between viscous dissipation and thermal conduction in Casson fluid flow. Higher Eckert values result into more significant initial temparature increases. After the initial rise, the temparature profiles decreases which emphasizes the influence of viscous effects on thermal properties of the fluid flow. Fig. 9 demonstrates the effect of varrying Prandlt number on temparature distributions which decreases nonuniformaly for increasing the Prandtl numbers (*Pr*).

5. Conclusion:

The analysis presents the following conclusions:

- The fluid velocity decreases as viscosity parameter decreases and the Casson fluid parameter increases.
- An increase in suction parameter leads to decrease in both velocity and temperature.
- An increase in Eckert number raises the initial temperature but eventually leads to decrease in the temperature profiles.
- An increase in magnetic and porosity parameters results into decrement in the fluid velocity.
- The velocity of the fluid decreases with increase in *Pr*.

5. References:

[1] L. Zheng , J. Niu, X. Zhang and L. Ma, "Dual solutions for flow and radiative heat transfer of a micropolar fluid over stretching/shrinking sheet", Int. J. Heat and Mass transfer, 55, 7577-7586 , (2012).

[2] B.C. Sakiadis, "Boundary layer behaviour on continuous solid surfaces", I: boundary-layer equations for two-dimensional and axisymmetric flow, AIChE J., 7 (1), 26-28, (1961).

[3] L. J. Crane, "Flow past a stretching plate", Zeitschrift fur Angewandte Mathematik und Physik (ZAMP), 21(4), 645–647, (1970).

[4] M. S. Abel and N. Mahesh, "Heat transfer in MHD viscoelastic fluid flow over a stretching sheet with variable thermal conductivity, non-uniform heat source and radiation", Applied Mathematical Modelling, 23(10), 1965-1983, (2008).

[5] K. Vajravelu and K.V. Prasad, "Keller box method and its application", Publisher: Walter de Gruyter GmbH and Co., 279-382.

[6] S. Mukhopadhyay and H.I. Andersson, "Effects of slip and heat transfer analysis of flow over an unsteady stretching surface", Heat Mass Transfer, 45, 1447–1452, (2009).

[7] A. Ishak, R. Nazar and I. Pop, "MHD Flow Towards a Permeable Surface with Prescribed Wall Heat Flux", Chinese Physical Society and IOP Publishing Ltd, 26 (2009).

[8] T.G. Fang, J. Zhang and S. S. Yao, "Slip Magnetohydrodynamic Viscous Flow over a Permeable Shrinking Sheet", Chinese Physical Society and IOP Publishing Ltd, 27(12), (2010).

[9] V.B. Awati, N. Maheshkumar and A. Wakif, "Haar wavelet scrutinization of heat and mass transfer features during the convective boundary layer flow of a nanofluid moving over a nonlinearly stretching sheet", Partial diff. Eq. in Appl. Mathematics, 4, 100192, (2021).

[10] M. Turkyilmazoglu, "Heat and mass transfer of MHD second order slip flow", Computers & Fluids, 71, 426–434, (2013).

[11] Van Gorder RA, E. Sweet and K. Vajravelu. "Nano Boundary layers over stretching surfaces", Common Nonlinear Sci. Numer. Simul., 15,1494-500, (2010).

[12] V. B. Awati and N. M. Bujurke. "Approximate analytical solutions of MHD flow of a viscous fluid on a nonlinear porous shrinking sheet", Bulletin of The International Mathematical Virtual Institute, 4, 145-155, (2014).

[13] K.V. Prasad, M.S. Abel and S. K. Khan, "Momentum and heat transfer in visco-elastic fluid flow in a porous medium over a non-isothermal stretching sheet", Int. J. Numerical Methods for Heat and Fluid flow, 10(8), 786-801, (2000).

[14] V.B. Awati and N. Maheshkumar, "Analysis of forced convection boundary layer flow and heat transfer past a semi-infinite static and moving flat plate using nanofluids by Haar wavelets", Journal of Nanofluids, 10(1), 106-117, (2021).

[15] Z. Abbas and T. Hayat, "Stagnation slip flow and heat transfer over a nonlinear stretching sheet", Numerical Methods for Partial Diff. Eq., 27(2), 302-314, (2011).

[16] S. Liao, "A new branch of solutions of boundary-layer flows over an impermeable stretched plate", Int. J. of heat and mass transfer, 48(12), 2529–2539, (2005).

[17] S Liao. "A new branch of solutions of boundary-layer flows over a permeable stretching plate", International Journal of Non-Linear Mechanics, 42(6), 819–830, (2007).

[18] M.J. Uddin, W.A. Khan and S. Norsarahaida, "g-Jitter Mixed Convective Slip Flow of Nanofluid past a Permeable Stretching Sheet Embedded in a Darcian Porous Media with Variable Viscosity", PLoS ONE, 9(6), e99384, (2014).

[19] K. V. Prasad, K. Vajravelu, H. Vaidya and R. A. Van Gorder, "MHD flow and heat transfer in a nanofluid over a slender elastic sheet with variable thickness", Results in Physics, 7, 1462-1474, (2017).

[20] V. B. Awati, S. S. Muchandi, N. Maheshkumar and A. Goravar, "Heat and mass transfer within MHD Williamson nanofluid flow under velocity and thermal slips in porous medium: numerical and semi-numerical approach", Canadian Transactions of Mathematical Computing, 1(1), 1-15, (2025).

[21] D. Ramya, R. S. Raju, J. A. Rao and A.J. Chamkha, "Effects of velocity and thermal wall slip on MHD boundary layer viscous flow and heat transfer of a nanofluid over a nonlinearly stretching sheet", Propulsion and power research, 7(2), 182-195, (2018).

[22] M. Mustafaa, T. Hayat, I. Pop and A. Hendi, "Stagnation-Point Flow and Heat Transfer of a Casson Fluid towards a Stretching Sheet", Zeitschrift fur Naturforschung 67a, 70 – 76, (2012).

[23] V. B. Awati, S. S. Muchandi, N. Maheshkumar, T. Muhammad, M. Zaydan, A. Wakif and R. Sehaqui, "New insights into transport phenomena within steady MHD two-phase nanofluid flows over a permeable elastic sheet of an uneven thickness", Modern Physics Letters B, 39(15), 2450488, (2025).

[24] V. B. Awati, S. S. Muchandi, N. Maheshkumar and G. Bognar, "Heat and mass transfer in MHD-UCM nanofluid

flow past a porous nonlinear stretching sheet with chemical reaction and bioconvection: a dual-method approach", Nanotechnology Reviews, 15(1), 20250251, (2026).

[25] R. Cortell, "Viscous flow and heat transfer over a nonlinearly stretching sheet", Applied Mathematics and Computation, 184, 864–873, (2007).

[26] F.C. Lai, F.A. Kulacki, "The effect of variable viscosity on convective heat transfer along a vertical surface in a saturated porous medium", Int. J Heat Mass Trans, 33, 1028-31, (1990).

[27] T.Y. Na, "Computational methods in engineering boundary value problems", Academic Press, New York, (1980).

*****